Table II. Results of the Correlations of the Relative Increase of Network Volume per Mole of Former Cation with the $\delta$ Index[a]

| glass system | parameters in eq 8 | | | | parameter $K'$ in eq 9 |
|---|---|---|---|---|---|
| | $K$ | $\beta$ | $S$ | $R$ | |
| $Li_2O$–$SiO_2$, 25 °C | 0.752 | 1.113 | 0.0053 | 0.9987 | 0.70 |
| $Na_2O$–$SiO_2$, 25 °C | 1.380 | 1.066 | 0.0074 | 0.9987 | 1.35 |
| $K_2O$–$SiO_2$, 25 °C | 2.260 | 1.034 | 0.0024 | 0.9999 | 2.27 |
| $Li_2O$–$SiO_2$, 1300 °C | 1.147 | 1.050 | 0.0029 | 0.9999 | 1.13 |
| $Na_2O$–$SiO_2$, 1300 °C | 1.851 | 0.975 | 0.0038 | 0.9999 | 1.99 |
| $K_2O$–$SiO_2$, 1300 °C | 3.057 | 1.005 | 0.0042 | 0.99996 | 3.22 |
| LiF–$BeF_2$, 20 °C | 0.730 | 1.044 | 0.0026 | 0.9999 | 0.73 |
| NaF–$BeF_2$, 20 °C | 1.027 | 1.059 | 0.0057 | 0.9996 | 1.02 |
| KF–$BeF_2$, 20 °C | 1.525 | 1.014 | 0.0066 | 0.9996 | 1.55 |
| RbF–$BeF_2$, 20 °C | 2.047 | 1.059 | 0.0090 | 0.9995 | 1.97 |

[a] S = standard deviation; R = correlation coefficient.

studied for several glass systems: LiF–$BeF_2$, NaF–$BeF_2$, KF–$BeF_2$, RbF–$BeF_2$ at 20 °C; $Li_2O$–$SiO_2$, $Na_2O$–$SiO_2$, $K_2O$–$SiO_2$ at 25 °C and at 1300 °C. The correlation of the relative increase of network volume per mole of former cation with the $\delta$ index for each system was calculated by the least-squares method. The number of glasses studied and the range of compositions covered for each system are shown in Table I. The values of $[V(x) - V(0)]/V(0)$ were calculated from the experimental data taken from the references listed in Table I, and the values of $\delta$ were calculated by using eq 7. In all cases the general form of a Walker-type equation[22] was obtained:

$$[V(x) - V(0)]/V(0) = K\delta^{\beta} \quad (8)$$

The results of these correlations are summarized in Table II.

Except for the $Li_2O$–$SiO_2$ system at 25 °C, the correlation coefficient exceeded 0.9995. These results are better than the correlations obtained on the basis of the number of edges only instead of the $\theta$ index.

All values of $\beta$ are very close to 1. That means that for a given glass system at a given temperature the relative increase of network volume per mole of former cation is practically proportional to the $\delta$ index. In spite of the fact that the hypothesis of a single value of $\beta$ for all the cases cannot be accepted statistically, eq 9,

$$[V(x) - V(0)]/V(0) = K'\delta^{1.038} \quad (9)$$

where $K'$ takes for each system the values listed in Table II, predicts the volume $V(x)$ of these glasses with an error less than 1.3% over the whole range of concentrations studied. If we compare glasses of the same group we observe that the constant $K'$ increases with the size of the modifier ions. This fact was expected from our previous statement about the location of these ions in the voids of the network.

It can also be observed that for the alkali silicate glasses, which have been studied at two different temperatures, the constant $K$ increases with temperature. Obviously, for the same degree of structural rigidity, the network expansion increases with the degree of thermal oscillation.

## Conclusions

In this paper we have illustrated the way in which graph theory can help us to study relationships between properties and structure for polymeric disordered structures. The results obtained for some inorganic glasses show a very simple relationship between the $\delta$ index (defined as a measure of the structural rigidity and directly related to the chemical composition) and the degree of expansion of the network due to the introduction of modifier ions.

**Registry No.** $SiO_2$, 7631-86-9; $BeF_2$, 7787-49-7.

# Theoretical Analysis of Acetyltriazene and the Mechanistic Implications of Its Reaction with Acid

**Judy L. Ozment,*,† Ann M. Schmiedekamp,† Laurie A. Schultz-Merkel,† Richard H. Smith, Jr.,‡ and Christopher J. Michejda*,§**

*Contribution from the Departments of Chemistry and Physics, Pennsylvania State University, Ogontz Campus, Abington, Pennsylvania 19001, Laboratory of Chemical and Physical Carcinogenesis, ABL-Basic Research Program, NCI-Frederick Cancer Research and Development Center, Frederick, Maryland 21702, and Department of Chemistry, Western Maryland College, Westminster, Maryland 21157.* *Received February 5, 1990*

**Abstract:** Theoretical calculations have been carried out on the protonation of 3-acetyltriazene in order to provide insight into the mechanism of the acid-catalyzed decomposition of acyltriazenes. We have previously reported the results of calculations on a series of alkyltriazenes. Ab initio RHF calculations were carried out at the 3-21G level to determine the optimized SCF energies and geometries of the neutral molecule and some site-specific protonated species. This allowed an estimate of the proton affinity at each site. Experimental studies on alkyltriazenes indicated that initial protonation at the $N_3$ site was critical in the acid catalysis mechanism, even though the calculated proton affinities indicated that $N_1$ was a more basic site. In the case of the acyltriazenes, the calculations showed that the proton affinity at $N_3$ was much lower than that at $N_1$ or at the carbonyl oxygens. The geometrical changes produced by protonations at the various sites indicated that the $N_2$–$N_3$ bond shows a propensity for cleavage upon protonation at either $N_3$ or at the carbonyl oxygen. These results suggest that acid-catalyzed decomposition of acetyltriazene would involve the breakage of the $N_2$–$N_3$ bond, rather than the hydrolysis of the acyl group. Subsequent experimental data supported this conclusion. A linear scaling method was applied to the geometric and energetic results from the semiempirical AM1 code to predict the results of the 3-21G calculations with a surprising degree of success. A predictor function to allow AM1 geometries and proton affinities to provide a good estimate of 3-21G results is given, and the limitations are discussed.

## I. Introduction

We initiated a theoretical study of various triazenes as a means of elucidating some of the mechanistic details of their aqueous decomposition reactions. Extensive laboratory studies have been carried out to improve the syntheses and document the decomposition kinetics of many representative members of the triazene family. The importance of these compounds stems from their ability to decompose into reactive diazonium ions. The alkyltriazenes undergo a specific acid-catalyzed decomposition to alkyldiazonium ions and the corresponding amines (eq 1).

† Pennsylvania State University.
‡ Western Maryland College.
§ NCI-Frederick Cancer Research and Development Center.

0002-7863/91/1513-397$02.50/0 

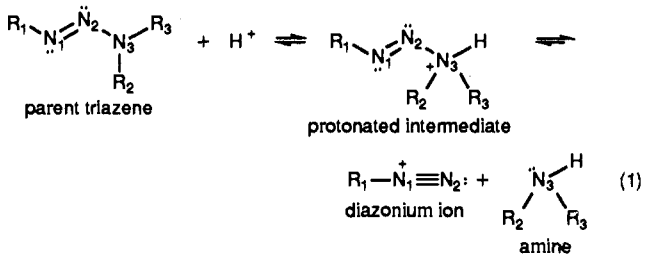


Diazonium ions are the putative ultimate carcinogens from a variety of carcinogenic substances, including *N*-nitroso compounds and alkylhydrazines.[1] Several 1-aryl-3,3-dialkyltriazenes have been shown to be mutagens and carcinogens,[2,3] as well as to possess antitumor properties,[4] and one, DTIC, is used clinically against some cancers.[5] The 1,3-dialkyltriazenes have been the subject of both theoretical[6] and experimental[7,8] studies. 1,3,3-Trialkyltriazenes have been synthesized,[9,10] and their aqueous decomposition has been examined.[11,12] As would be expected from their chemical behavior, aliphatic triazenes exhibit potential biological activity without the necessity of enzymatic activation systems. The di- and trialkyltriazenes were shown to be potent mutagens[13] and capable of alkylating DNA in vitro and in vivo.[14] One member of the series, 1,3-diethyltriazene, was found to be a carcinogen in rats.[15] The extreme lability of the alkyltriazenes toward aqueous decomposition made their use somewhat limited in further biological applications.

Acyltriazenes were developed in an effort to devise more stable compounds, the rationale being that the electronegative group on $N_3$ would slow the rate of acid-catalyzed decomposition. In fact, the acyltriazenes were found to be much more stable than their alkyl analogues, but the mechanism of their decomposition proved to be much more complex.[7] Detailed examination of the hydrolytic decomposition of 3-carboethoxy-1,3-dimethyltriazene (DMC), 3-(diethoxyphosphinyl)-1,3-dimethyltriazene (DMP), 3-*N*-methylcarbamoyl-1,3-dimethyltriazene (DMM), and 3-acetyl-1,3-dimethyltriazene (DMA) (see Figure 1) showed the reaction proceeded by at least three different mechanisms, which depend on the pH of the medium. In general, there was an acid-catalyzed reaction, a neutral uncatalyzed reaction, and a base-catalyzed reaction. The mechanism of the acid-catalyzed reaction could be envisioned as involving the hydrolysis of the acyl substituent (breaking the $N_3$–P or $N_3$–C bond; see Figure 1), resulting in the formation of the dimethyltriazene. An alternative pathway would involve the direct dissociation of the protonated triazene to produce

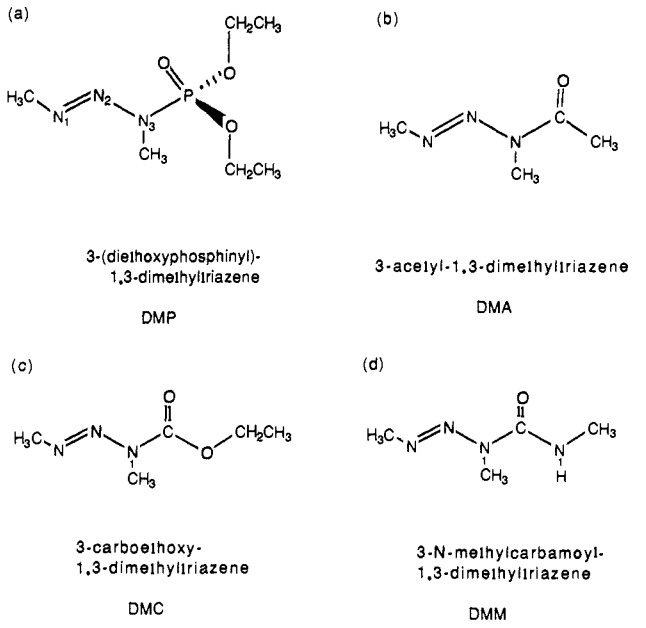


Figure 1. The acyltriazenes investigated experimentally.[7]

the methyldiazonium ion (by breaking the $N_2$–$N_3$ bond; see Figure 1) and the corresponding amide. Recent experimental evidence indicates that the acid-catalyzed reaction of all the acyltriazenes (DMA, DMC, DMP, and DMM) occurs by the second pathway, as the unhydrolyzed amides were recovered in virtually quantitative yields from the decomposition reactions.[16] In solutions of pH 4–8, the reaction is thought to occur by a slow direct $N_2$–$N_3$ dissociation to produce the methyldiazonium ion and the amidyl anion, with no proton present in the transition state.[7]

Prior to this investigation, ab initio restricted Hartree–Fock (RHF) molecular orbital calculations for proton affinity were carried out on unsubstituted triazene (see eq 1, with $R_1 = R_2 = R_3 = H$), 1-methyltriazene ($R_1 = Me$, $R_2 = R_3 = H$), and 1,3-dimethyltriazene ($R_1 = R_2 = Me$, $R_3 = H$).[6,17,18] Some preliminary work has been done to relate the ability of the semiempirical AM1 code to reproduce the ab initio RHF results for the triazene systems.[19] A comparison of AM1 to the ab initio results is considered important for large molecules. The ab initio RHF calculations for such molecules become prohibitively large. AM1 has been known to have some difficulty reproducing results determined by ab initio methods, but there is growing evidence that it can follow the *trends* of ab initio calculations. Promising results were found for triazene and alkyltriazenes: the AM1 code predicted trends in the proton affinities of various sites in the triazenes, though the actual AM1 proton affinity values were lower than those obtained by ab initio methods. One of our ongoing objectives is to assess the reliability of the semiempirical AM1 code and to create a simple algorithm that will adjust the AM1 results.

The theoretical analysis reported here was designed to determine whether acyltriazenes decompose in acid by $N_2$–$N_3$ bond cleavage or by the $N_3$–C hydrolysis (deacylation). Additionally, we hoped to characterize the reduced reactivity of acyltriazenes, as compared with alkyltriazenes. Finally, we hoped to determine a suitable method by which to use semiempirical results to predict ab initio RHF results, so that those less expensive calculations can be predictive of both ab initio results, as well as experimental findings. These goals were accomplished by determining the proton affinity as a measure of the relative potential for protonation of various sites of an acyltriazene molecule, and by investigating the structural changes that occur when the molecule is protonated.

(1) Smith, R. H., Jr.; Koepke, S. R.; Tondeur, Y.; Denlinger, C. L.; Michejda, C. J. *J. Chem. Soc., Chem. Commun.* **1985**, 936–8.
(2) (a) Malaveille, C.; Kolar, G. F.; Bartsch, H. *Mutat. Res.* **1976**, *36*, 1–10. (b) Kolar, G. F.; Fahrig, R.; Vogel, E. *Chem.-Biol. Interact.* **1974**, *9*, 365–78.
(3) Preussmann, R.; Ivankovic, S.; Landschutz, C.; Gurmy, J.; Flohr, E.; Griesbach, U. *Z. Krebsforsch. Clin. Onkol.* **1974**, *81*, 285–310.
(4) Clark, D. A.; Barclay, R. K.; Stock, C. C.; Rondesvedt, C. S., Jr. *Proc. Soc. Exptl. Biol. Med.* **1955**, *90*, 484–8.
(5) Comis, R. L. *Cancer Treat. Rep.* **1976**, *60*, 165–76.
(6) Schmiedekamp, A.; Smith, R. H., Jr.; Michejda, C. J. *J. Org. Chem.* **1988**, *53*, 3433–6.
(7) Smith, R. H., Jr.; Mehl, A. F.; Hicks, A.; Denlinger, C. L.; Kratz, L.; Andrews, A. W.; Michejda, C. J. *J. Org. Chem.* **1986**, *51*, 3751.
(8) Smith, R. H., Jr.; Wladkowski, B. D.; Mehl, A. F.; Cleveland, M. J.; Rudrow, E. A.; Chmurny, G. H.; Michejda, C. J. *J. Org. Chem.* **1989**, *54*, 1036–1042.
(9) Sieh, D. H.; Wilbur, D. J.; Michejda, C. J. *J. Am. Chem. Soc.* **1980**, *102*, 3883–7.
(10) Smith, R. H., Jr.; Michejda, C. J. *Synthesis* **1983**, 476–7.
(11) Sieh, D. H.; Michejda, C. J. *J. Am. Chem. Soc.* **1981**, *103*, 442–5.
(12) Smith, R. H., Jr.; Denlinger, C. L.; Kupper, R.; Koepke, S. R.; Michejda, C. J. *J. Am. Chem. Soc.* **1984**, *106*, 1056–9.
(13) Sieh, D. H.; Andrews, A. W.; Michejda, C. J. *Mutat. Res.* **1980**, *73*, 227–235.
(14) Smith, R. H., Jr.; Kroeger-Koepke, M. B.; Michejda, C. J., manuscript in preparation.
(15) Smith, R. H., Jr.; Kovatch, R. M.; Lijinsky, W.; Thomas, B. J.; Michejda, C. J. *Cancer Lett.* **1987**, *35*, 129–132.
(16) Smith, R. H., Jr.; Hurling, H. E.; Wladkowski, B. D.; Michejda, C. J., manuscript in preparation.
(17) Nguyen, M.-T.; Kaneti, J.; Hoesch, L.; Dreiding, A. S. *Helv. Chim. Acta* **1984**, *67*, 1618–1929.
(18) Nguyen, M.-T.; Hoesch, L. *Helv. Chim. Acta* **1986**, *69*, 1627–37.
(19) Schmiedekamp, A. M.; Ozment, J. L., manuscript in preparation.

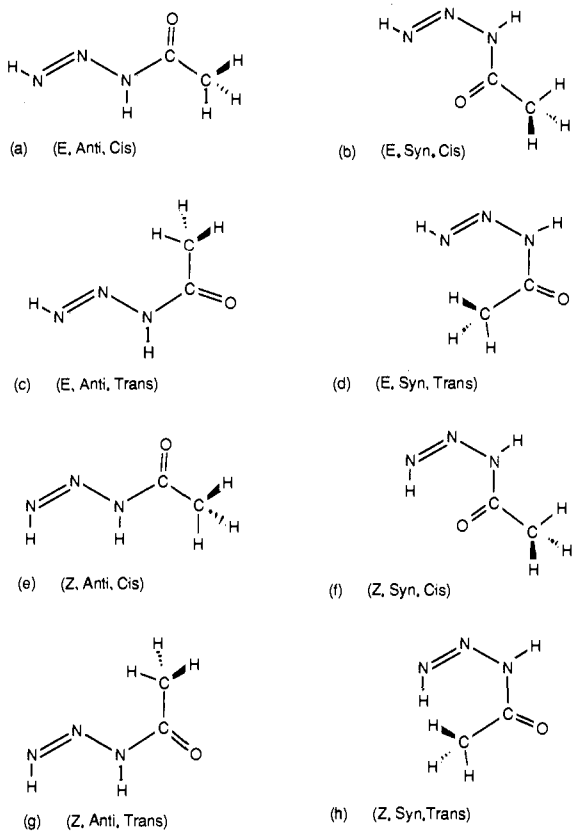


**Figure 2.** The eight coplanar conformations of 3-acetyltriazene.

## II. Theoretical Methods

We chose to analyze the 3-acetyltriazene molecule:

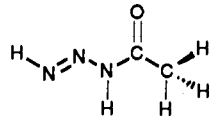

as a prototype for other acyltriazenes. In order to reduce the number of calculations, all of the calculations were initiated with a coplanar $\pi$-system. Our previous experience with alkyltriazene calculations indicates that nonplanar $\pi$-systems were energetically unfavorable. This yielded the set of eight conformers shown in Figure 2. We did not constrain any of the geometrical parameters, so subsequent optimization could still access asymmetric and nonplanar geometries.

We used the AM1 semiempirical code to do preliminary calculations using AMPAC[20] on an IBM 3090, to help make the process sensible in both time and cost. All AM1 results were obtained under the PRECISE option, to provide the strictest convergence criterion. The recent work of Boyd et al. indicates that this is essential.[21] By using the AM1 geometrical output as input to the ab initio restricted Hartree–Fock (RHF) calculations, each of the eight coplanar conformers (see Figure 2) of acetyltriazene were optimized at the 3-21G level on the Cray X-MP version of GAUSSIAN 82.[22] This provided us with conformation-specific SCF-optimized energies and conformational geometries. Similarly, ab initio RHF calculations were performed for each conformation protonated at the three most electronegative sites ($N_1$, $N_3$, and the carbonyl oxygen). To assure that these structures were true local minima, we checked the bond frequencies to see that they had positive values. The oxygen protonated structures were done at two different orientations, inferring protonation at each of the two nonbonding electron pairs of that oxygen. As an example, Figure 3 shows the four protonations of the acetyltriazene molecule in the conformation designated the (E,anti,cis) conformer (from Figure 2a).

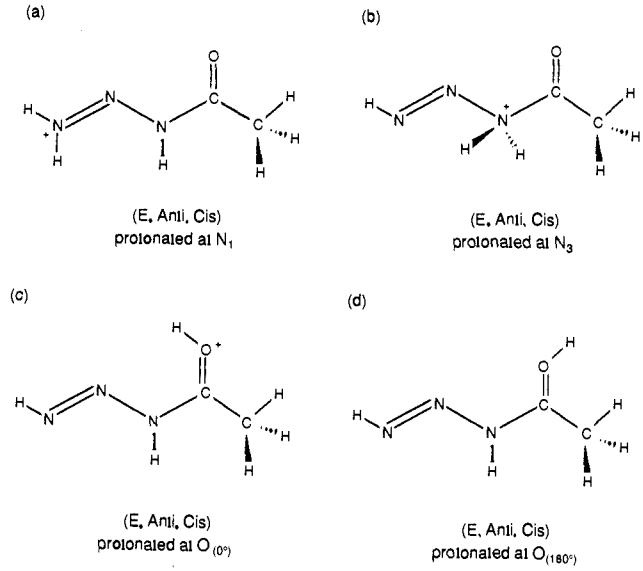


**Figure 3.** Protonation of 3-acetyltriazene at $N_1$ and $N_3$, and two oxygen protonations, $O_{(0°)}$ and $O_{(180°)}$. Each oxygen protonation is designated by the dihedral twist of $H^+$–O–C–$N_3$.

**Table I.** Conformation-Specific SCF Energies of Neutral 3-Acetyltriazene

| conformation[a] | 3-21G formation energies (hartrees)[b] | (kcal/mol)[c] | Z – E[d] | AM1 $\Delta H_f$ (kcal/mol)[e] |
|---|---|---|---|---|
| (E,anti,cis) | −314.998 757 2 | 2.44 | | 14.28 |
| (E,anti,trans) | −315.002 643 1 | 0.00 | | 11.91 |
| (E,syn,cis) | −314.987 812 7 | 9.31 | | 12.73 |
| (E,syn,trans) | −314.992 708 4 | 6.23 | | 9.99 |
| (Z,anti,cis) | −314.984 423 9 | 11.43 | 8.99 | 11.86 |
| (Z,anti,trans) | −314.992 037 8 | 6.65 | 6.65 | 8.04 |
| (Z,syn,cis) | −314.995 238 6 | 4.65 | −4.66 | 3.44 |
| (Z,syn,trans) | −314.975 506 2 | 17.10 | 10.89 | 7.30 |

[a] For conformation vocabulary, see Figure 2. [b] 3-21G basis set; SCF energy of optimized neutral geometry. [c] SCF energies above the lowest energy conformation, (E,anti,trans), converted to kcal/mol. [d] The difference between the Z-isomer SCF energy and the E-isomer SCF energy in kcal/mol. [e] AM1 optimized heats of formation.

The adequacy of the 3-21G basis set to predict correct proton affinity trends has been previously demonstrated. There, Schmiedekamp et al.[6] showed that the 3-21G level proton affinities of triazenes were consistently over-estimated relative to those calculated at the 6-31G* and MP3/6-31G* levels, but that the trends were parallel. Furthermore, Schmiedekamp and Ozment[19] demonstrated that the ab initio proton affinities at 3-21G are parallel in trend to the proton affinities at 3-21G$^+$, which is widely known to be reliable.[23]

The proton affinity is defined as the energy released in the protonation reaction:

$$\text{neutral} + H^+ \rightarrow \text{cation} \qquad (2)$$

Ab initio proton affinities were determined by subtracting the RHF–SCF energy of the neutral conformer from the RHF–SCF energy of the cation. AM1 proton affinities were calculated as the negative of the heat of the protonation reaction, so,

$$\text{proton affinity} = -[\Delta H_{f,\text{cation}} - \Delta H_{f,\text{neutral}} - \Delta H_{f,H^+}] \qquad (3)$$

where $\Delta H_{f,\text{cation}}$ is the heat of formation of the protonated species,

(20) Dewar, M. J. S.; Zoebisch, E. G.; Healy, E. F.; Stewart, J. J. P. *J. Am. Chem. Soc.* **1985**, *107*, 3902.
(21) Boyd, D. R.; Smith, D. W.; Stewart, J. J. P.; Wimmer, E. *J. Comput. Chem.* **1988**, *9*, 387–98.
(22) Binkley, J. S.; Whiteside, R. A.; Raghavachari, K.; Seeger, R.; DeFrees, D. J.; Schlegel, H. B.; Frisch, M. J.; Pople, J. A.; Kahn, L. R. GAUSSIAN 82, Carnegie-Mellon University, Pittsburgh, PA, 1982.

(23) (a) Hehre, W. J.; Radom, L.; Schleyer, P. v. R.; Pople, J. A. *Ab Initio Molecular Orbital Theory*; Wiley: New York, 1986; pp 310–315. (b) Sanz, J. F.; Anguiano, J. *J. Comput. Chem.* **1988**, *9*, 784–9.

Table II. Geometrical Parameters for ab Initio Neutral 3-Acetyltriazene

| | bond distances[a] (Å) | | | | |
|---|---|---|---|---|---|
| conformation | $N_1$–$N_2$ | $N_2$–$N_3$ | $N_3$–C | C–O | C–C |
| (E,anti,cis) | 1.236 | 1.385 | 1.378 | 1.206 | 1.514 |
| (E,anti,trans) | 1.236 | 1.378 | 1.378 | 1.211 | 1.508 |
| (E,syn,cis) | 1.232 | 1.396 | 1.385 | 1.205 | 1.520 |
| (E,syn,trans) | 1.235 | 1.384 | 1.392 | 1.213 | 1.503 |
| (Z,anti,cis) | 1.229 | 1.401 | 1.386 | 1.204 | 1.514 |
| (Z,anti,trans) | 1.230 | 1.393 | 1.384 | 1.210 | 1.505 |
| (Z,syn,cis) | 1.226 | 1.449 | 1.361 | 1.223 | 1.512 |
| (Z,syn,trans) | 1.228 | 1.419 | 1.387 | 1.212 | 1.509 |

| | bond angles[b] (deg) | | | | | |
|---|---|---|---|---|---|---|
| conformation | $HN_1N_2$ | $N_1N_2N_3$ | $N_2N_3H$ | $N_2N_3C$ | $N_3CO$ | $N_3CC$ |
| (E,anti,cis) | 108.6 | 112.0 | 116.1 | 120.1 | 123.4 | 112.3 |
| (E,anti,trans) | 108.6 | 112.8 | 117.7 | 121.5 | 120.1 | 115.6 |
| (E,syn,cis) | 107.5 | 116.3 | 110.2 | 130.4 | 125.5 | 111.1 |
| (E,syn,trans) | 107.9 | 116.8 | 111.5 | 133.4 | 117.5 | 119.3 |
| (Z,anti,cis) | 115.1 | 117.6 | 118.9 | 119.7 | 123.3 | 112.2 |
| (Z,anti,trans) | 114.7 | 118.5 | 120.6 | 121.1 | 119.6 | 115.6 |
| (Z,syn,cis) | 115.3 | 118.5 | 110.4 | 128.2 | 122.7 | 114.1 |
| (Z,syn,trans) | 116.8 | 122.5 | 109.0 | 137.2 | 118.4 | 119.7 |

[a] Not shown: H–N distances (1.015–1.026 Å) and H–C distances (1.078–1.084 Å). [b] Not shown: HCC angles (106.9°–111.3°), and all dihedral twist angles are within 1° of nominal.

$\Delta H_{f,neutral}$ is the heat of formation of the neutral molecule, and $\Delta H_{f,H^+}$ is the experimental value of the proton's heat of formation, 367.2 kcal/mol.[24]

## III. Results and Discussion

**A. Mechanistic Implications of the ab Initio Results. 1. Conformational Energies.** Ab initio RHF conformation-specific "gas-phase" energies of 3-acetyltriazene, optimized with the standard 3-21G basis set, are listed in Table I. From these data, we determine that the most energetically stable ab initio conformation is the (E,anti,trans) conformer. For ease of comparison, we give a list of conformation energies for the other seven conformations relative to the (E,anti,trans) energy. Though the (E,anti,trans) conformer has the lowest energy, the (E,anti,cis) conformer is only 2.44 kcal/mol higher, and all conformation energies are within 18 kcal/mol.

With only one exception, the ab initio RHF results indicate that the E-isomer energies are lower than those of the Z isomer by 6–11 kcal/mol; hence, these isomers are more stable in the gas phase. We show these differences for each conformation in Table I. This is probably explainable by the destabilization caused by the presence of the antiperiplanar lone pair on $N_1$ in Z isomers, as discussed earlier.[6] Only one exception arises with the (Z,syn,cis) conformer. It is more energetically stable than its E counterpart, the (E,syn,cis) conformer. Inspection of Figure 2, b and f, shows that the (Z,syn,cis) conformer is able to take advantage of intramolecular hydrogen bonding between the $N_1$ hydrogen and the carbonyl oxygen; this is not possible in the E isomer.

It is important to remember that conformers which may be most energetically stable in the gas phase, may not be the most stable in polar solvents. The relative order of conformers from a gas-phase calculation do not allow us to exclude certain conformations from consideration in solution. The solvent environment will be quite different from the gas phase. Consequently, the solvent interactions will stabilize some of the conformations better than others. For instance, the (Z,syn,cis) conformer is not likely to be stabilized as strongly as the E analogue by surrounding solvent molecules since the intramolecular hydrogen bond precludes interactions with the solvent. Although the calculations indicate this conformer is lower in energy than many of the others, we cannot necessarily assume that this order will be maintained in solution. In spite of this caveat, the gas-phase calculations provide a useful benchmark for understanding the effect of protonation on triazene decomposition.

**2. Conformational Geometries.** Table II provides the essential geometrical results from the ab initio RHF calculation of the eight neutral conformations. In each conformation, the molecule starts out with the $N_1$–$N_2$ bond length shorter than $N_2$–$N_3$, reminiscent of the structures shown in Figure 2. The $N_2$–$N_3$ bond lengths are between the normal N–N single bond length (considered to be about 1.45–1.48 Å)[25] and double bond length (considered to be about 1.22–1.23 Å).[25] The $N_3$–C bond lengths are also smaller than the normal single bond length (considered to be about 1.47–1.51 Å).[25] The optimized molecule remained coplanar in all of the conformations; all flat dihedral angles were within 1° of planar. These attributes all suggest that there is some degree of resonance through the nitrogen lone electron pair connecting the two $\pi$-bonds of this molecule. Almost all the angles are within 5° of nominal. The $HN_1N_2$ angle, however, was found to be quite narrow. The lone-pair repulsion interaction with the H–$N_1$ $\sigma$-bonding electrons is greater than the repulsion interaction of H–$N_1$ and $N_1$–$N_2$ bonding electrons. It is interesting to note that the Z isomers have a significantly wider $HN_1N_2$ angle than those of E isomers, in every case.

Pronounced variations appeared in the $N_2N_3H$ and $N_2N_3C$ angles of all syn conformations. The $N_2N_3H$ angles were narrow and the $N_2N_3C$ angles were wide. This is probably a result of steric strain (see Figure 2, c, d, g, and h). Also, in all cis conformations, the $N_3CC$ angles were narrower than in the corresponding trans conformations, and the $N_3CO$ angles were wider. In the cis conformations (see Figure 2, a, b, e, and f), the oxygen lone electron pair in the plane of the triazene may experience some repulsion from the nitrogen lone electron pair also in that plane. The molecule will adjust by tilting the acetyl group away from the triazene, increasing the NCO angle and decreasing the NCC angle. Each of these effects causes minor structural variations in the conformational geometries.

Table III provides the essential geometrical results from the ab initio RHF calculation of 3-acetyltriazene protonated at four sites: $N_1$, $N_3$, and the two oxygen orientations. As with the neutrals, these were calculated with the standard 3-21G basis set. Notice that protonation at the oxygen site [$O_{(0°)}$] relieves the electronically induced tilting of the acetyl group in the cis conformations, and that protonations of the syn conformations still retained significant angle distortions due to steric crowding. There were five calculations that could not be optimized; hence the data for all Z isomers protonated at $N_3$ and both oxygen protonations of the (Z,syn,cis) conformer are not given in Table III. In all five cases, the optimization calculations produced the same symptoms

(24) Aue, D. H.; Bowers, M. T. Stabilities of positive ions from equilibrium gas-phase basicity measurements; In *Gas Phase Ion Chemistry*; Bowers, M. T., Ed., Academic: New York, 1979; Vol. 2.

(25) March, J. *Advanced Organic Chemistry*; Wiley: New York, 1985; p 19.

**Table III.** Important Bond Distances and Angles for the ab Initio 3-Acetyltriazenes Protonated at $N_1$, $N_3$, and Two Oxygen Orientations

| conformation | protonation site[a] | bond distances[b] (Å) | | | |
|---|---|---|---|---|---|
| | | $N_1$–$N_2$ | $N_2$–$N_3$ | $N_3$–C | C–O |
| (E,anti,cis) | $N_1$ | 1.270 L[c] | 1.278 S[c] | 1.494 L | 1.183 S |
| | $N_3$ | 1.206 S | 1.567 L | 1.582 L | 1.174 S |
| | $O_{(0°)}$ | 1.219 S | 1.444 L | 1.300 S | 1.294 L |
| | $O_{(180°)}$ | 1.219 S | 1.461 L | 1.290 S | 1.297 L |
| (E,anti,trans) | $N_1$ | 1.273 L | 1.270 S | 1.488 L | 1.187 S |
| | $N_3$ | 1.209 S | 1.545 L | 1.600 L | 1.176 S |
| | $O_{(0°)}$ | 1.218 S | 1.458 L | 1.296 S | 1.303 L |
| | $O_{(180°)}$ | 1.219 S | 1.448 L | 1.290 S | 1.303 L |
| (E,syn,cis) | $N_1$ | 1.258 L | 1.309 S | 1.440 L | 1.205 |
| | $N_3$ | 1.198 S | 1.590 L | 1.597 L | 1.173 S |
| | $O_{(0°)}$ | 1.225 S | 1.440 L | 1.317 S | 1.283 L |
| | $O_{(180°)}$ | 1.214 S | 1.478 L | 1.296 S | 1.294 L |
| (E,syn,trans) | $N_1$ | 1.270 L | 1.279 S | 1.488 L | 1.188 S |
| | $N_3$ | 1.203 S | 1.560 L | 1.640 L | 1.174 S |
| | $O_{(0°)}$ | 1.214 S | 1.474 L | 1.302 S | 1.308 L |
| | $O_{(180°)}$ | 1.217 S | 1.458 L | 1.297 S | 1.307 L |
| (Z,anti,cis) | $N_1$ | 1.270 L | 1.278 S | 1.494 L | 1.183 S |
| | $N_3$[d] | (S) | (L) | (L) | (S) |
| | $O_{(0°)}$ | 1.209 S | 1.481 L | 1.307 S | 1.290 L |
| | $O_{(180°)}$ | 1.203 S | 1.528 L | 1.294 S | 1.295 L |
| (Z,anti,trans) | $N_1$ | 1.273 L | 1.270 S | 1.488 L | 1.187 S |
| | $N_3$[d] | (S) | (L) | (L) | (S) |
| | $O_{(0°)}$ | 1.203 S | 1.517 L | 1.300 S | 1.304 L |
| | $O_{(180°)}$ | 1.207 S | 1.496 L | 1.294 S | 1.303 L |
| (Z,syn,cis) | $N_1$ | 1.258 L | 1.309 S | 1.440 L | 1.205 S |
| | $N_3$[d] | (S) | (L) | (L) | (L) |
| | $O_{(0°)}$[d] | (S) | (L) | (S) | (L) |
| | $O_{(180°)}$[d] | (S) | (L) | (S) | (L) |
| (Z,syn,trans) | $N_1$ | 1.270 L | 1.279 S | 1.488 L | 1.188 S |
| | $N_3$[d] | (S) | (L) | (L) | (S) |
| | $O_{(0°)}$ | 1.168 S | 1.687 L | 1.283 S | 1.317 L |
| | $O_{(180°)}$ | 1.189 S | 1.595 L | 1.285 S | 1.312 L |

| conformation | protonation site[a] | bond angles[f] (deg) | | | | | | |
|---|---|---|---|---|---|---|---|---|
| | | $HN_1N_2$ | $N_1N_2N_3$ | $N_2N_3H$ | $N_2N_3C$ | $N_3CO$ | $N_3CC$ | new H[c] |
| (E,anti,cis) | $N_1$ | 115.8 L[d] | 120.7 L | 121.8 L | 117.7 L | 117.9 S | 111.1 S | 124.1 |
| | $N_3$ | 111.3 S[d] | 107.5 S | 107.7 S | 109.7 S | 116.4 S | 110.6 S | 107.7 |
| | $O_{(0°)}$ | 110.8 L | 110.6 S | 117.7 L | 117.4 S | 120.9 S | 121.7 L | 118.0 |
| | $O_{(180°)}$ | 110.4 L | 108.3 S | 115.7 S | 120.6 L | 117.2 S | 119.9 L | 119.4 |
| (E,anti,trans) | $N_1$ | 116.1 L | 120.6 L | 123.0 L | 121.3 S | 114.2 S | 115.0 S | 123.6 |
| | $N_3$ | 111.4 L | 108.2 S | 108.5 S | 113.4 S | 113.1 S | 113.3 S | 108.5 |
| | $O_{(0°)}$ | 110.7 L | 109.1 S | 115.3 S | 118.7 S | 121.9 L | 121.3 L | 121.3 |
| | $O_{(180°)}$ | 110.5 L | 109.4 S | 117.9 L | 119.5 S | 114.8 S | 122.1 L | 119.3 |
| (E,syn,cis) | $N_1$ | 115.3 L | 120.7 L | 112.4 L | 126.6 S | 118.1 S | 113.4 L | 121.6 |
| | $N_3$ | 111.1 L | 111.6 S | 102.1 S | 125.1 S | 119.0 S | 108.9 L | 102.2 |
| | $O_{(0°)}$ | 110.8 L | 113.2 S | 110.7 L | 128.1 S | 122.2 S | 119.8 L | 116.0 |
| | $O_{(180°)}$ | 109.3 L | 113.8 S | 107.8 S | 132.4 L | 119.3 S | 118.7 L | 119.0 |
| (E,syn,trans) | $N_1$ | 114.9 L | 123.8 L | 112.1 L | 136.2 L | 113.1 S | 118.9 S | 125.0 |
| | $N_3$ | 110.7 L | 111.8 S | 103.1 S | 130.0 S | 110.2 S | 116.2 S | 103.1 |
| | $O_{(180°)}$ | 110.0 L | 113.2 S | 107.5 S | 130.8 S | 120.1 L | 126.1 L | 121.3 |
| | $O_{(180°)}$ | 109.8 L | 113.2 S | 110.3 S | 131.4 S | 112.9 S | 125.9 L | 119.2 |
| (Z,anti,cis) | $N_1$ | 124.1 L | 120.7 L | 121.8 L | 117.7 L | 117.9 S | 111.1 S | 115.8 |
| | $N_3$ | | | | | | | |
| | $O_{(0°)}$ | 119.5 L | 118.0 L | 122.7 L | 114.9 S | 120.9 S | 121.7 L | 118.0 |
| | $O_{(180°)}$ | 121.2 L | 114.8 L | 120.8 L | 118.3 S | 120.9 S | 120.3 L | 118.0 |
| (Z,anti,trans) | $N_1$ | 123.6 L | 120.6 L | 123.0 L | 121.3 S | 114.2 S | 115.0 S | 116.1 |
| | $N_3$[e] | | | | | | | |
| | $O_{(0°)}$ | 121.0 L | 116.0 S | 120.6 | 116.1 S | 122.2 L | 122.5 L | 121.5 |
| | $O_{(180°)}$ | 120.1 L | 116.2 S | 122.9 L | 117.1 S | 114.8 S | 122.3 L | 119.4 |
| (Z,syn,cis) | $N_1$ | 121.6 L | 120.7 L | 112.4 L | 126.6 S | 118.1 S | 113.4 L | 115.3 |
| | $N_3$[e] | | | | | | | |
| | $O_{(0°)}$[e] | | | | | | | |
| | $O_{(180°)}$[e] | | | | | | | |
| (Z,syn,trans) | $N_1$ | 125.0 L | 123.8 L | 112.1 L | 136.2 L | 113.1 S | 118.9 S | 114.9 |
| | $N_3$[e] | | | | | | | |
| | $O_{(0°)}$ | 128.4 L | 117.7 S | 102.6 S | 136.4 S | 123.4 L | 123.8 L | 120.0 |
| | $O_{(180°)}$ | 124.5 L | 118.9 S | 105.3 S | 137.5 L | 114.9 S | 124.2 L | 119.6 |

[a] Each oxygen protonation is designated by the dihedral twist angle of $H^+$–O–C–$N_3$; see Figure 3. [b] Angles not shown: HCC angles (106.9–111.3°) and all dihedral twist angles within 1° of nominal. [c] New H is the proton at the designated protonation site; see Figure 3. [d] S = smaller than its neutral counterpart. L = larger than its neutral counterpart. [e] 3-21G calculations did not optimize for these conformational protonations. [f] Distances not shown: H–N distances (1.001–1.023 Å), H–C distances (1.077–1.085 Å), and C–C distances (1.317–1.598 Å, most near 1.490 Å).

Table IV. Conformation-Specific and Protonation Site-Specific Proton Affinities of 3-Acetyltriazene

| | proton affinity (kcal/mol) | | | | | | | |
|---|---|---|---|---|---|---|---|---|
| | 3-21G at each protonation site | | | | AM1 at each protonation site | | | |
| conformation | $N_1$ | $N_3$ | $O_{(0°)}$[a] | $O_{(180°)}$[a] | $N_1$ | $N_3$ | $O_{(0°)}$ | $O_{(180°)}$ |
| (E,anti,cis) | 217.9 | 194.9 | 221.6 | 216.3 | 202.7 | 187.5 | 202.6 | 198.9 |
| (E,anti,trans) | 216.6 | 193.3 | 214.0 | 216.8 | 201.1 | 185.1 | 198.0 | 198.6 |
| (E,syn,cis) | 234.6 | 197.3 | 227.7 | 216.2 | 209.1 | 187.0 | 203.2 | 201.3 |
| (E,syn,trans) | 213.8 | 194.8 | 213.8 | 217.1 | 198.5 | 184.3 | 199.0 | 199.9 |
| (Z,anti,cis) | 226.9 | *b* | 219.7 | 212.5 | 202.7 | 183.2 | 204.3 | 199.8 |
| (Z,anti,trans) | 223.2 | *b* | 208.5 | 212.6 | 201.1 | 181.3 | 198.1 | 199.4 |
| (Z,syn,cis) | 230.0 | *b* | *b* | *b* | 209.1 | 183.4 | 195.9 | 196.5 |
| (Z,syn,trans) | 225.2 | *b* | 209.0 | 209.5 | 198.5 | 180.4 | 195.9 | 196.0 |

[a] Each oxygen protonation is designated by the dihedral twist angle for $H^+$–O–C–$N_3$; see Figure 3. [b] 3-21G calculations did not optimize for the protonated form involved here, so no proton affinity could be calculated.

Table V. Linear Fit Parameters[a] for Some Geometry Scaling, Comparing AM1 Results with ab Initio Results

| | proton affinity (kcal/mol) | | | | | | | |
|---|---|---|---|---|---|---|---|---|
| | 3-21G at each protonation site | | | | AM1 at each protonation site | | | |
| conformation | $N_1$ | $N_3$ | $O_{(0°)}$[a] | $O_{(180°)}$[a] | $N_1$ | $N_3$ | $O_{(0°)}$ | $O_{(180°)}$ |
| (E,anti,cis) | 217.9 | 194.9 | 221.6 | 216.3 | 202.7 | 187.5 | 202.6 | 198.9 |
| (E,anti,trans) | 216.6 | 193.3 | 214.0 | 216.8 | 201.1 | 185.1 | 198.0 | 198.6 |
| (E,syn,cis) | 234.6 | 197.3 | 227.7 | 216.2 | 209.1 | 187.0 | 203.2 | 201.3 |
| (E,syn,trans) | 213.8 | 194.8 | 213.8 | 217.1 | 198.5 | 184.3 | 199.0 | 199.9 |
| (Z,anti,cis) | 226.9 | *b* | 219.7 | 212.5 | 202.7 | 183.2 | 204.3 | 199.8 |
| (Z,anti,trans) | 223.2 | *b* | 208.5 | 212.6 | 201.1 | 181.3 | 198.1 | 199.4 |
| (Z,syn,cis) | 230.0 | *b* | *b* | *b* | 209.1 | 183.4 | 195.9 | 196.5 |
| (Z,syn,trans) | 225.2 | *b* | 209.0 | 209.5 | 198.5 | 180.4 | 195.9 | 196.0 |

[a] Fit to $y_{bond} = mx_{bond} + b$, for $x_{bond}$ = (AM1 optimized geometry) and $y_{bond}$ = (3-21G optimized geometry). [b] See footnote *b* in Table IV.

in the $N_3$ protonation of the (*Z*)-triazene.[6] At each step of the calculation the $N_2$–$N_3$ bond grew longer, and no stationary state was reached. In each case, the $N_2$–$N_3$ length was much longer than a single bond in the final nonoptimized geometry (as high as 2.5 Å).

It is speculation at this point to consider that the unconverged 3-21G optimization actually implies irreversible bond cleavage, but in several other ongoing tests on similar systems, there is additional evidence that some of the protonations caused the molecule to become unstable enough so that an energy minimum was not found. We were unsuccessful in reaching RHF convergence at the 3-21G level on the $N_3$ protonated unsubstituted (*Z*)-triazene, even calculating the force constants analytically at each step. A 6-31G* calculation with a standard Berny optimization on the unsubstituted triazene did result in a stationary state with a noticeably large $N_2$—$N_3$ bond of 1.599 Å and a tight $N_1$=$N_2$ bond of 1.174 Å. Considering this geometry, it would be easy to believe that this was a shallow intermediate form, rather than a true global minimum. At the optimized 6-31G* geometry, the $N_3$ had a charge excess of 0.79 (calculated from Mulliken population analysis), indicating a partial transfer of electrons to it from $N_2$, reminiscent of the electron transfer that does occur during the heterolysis of $N_2$–$N_3$ bond. Calculations were also performed on the (Z,anti,cis) conformer of 3-formyltriazene protonated on $N_3$. An energy minimum was not located in this case, at either 3-21G or 6-31G* using the Berny optimization. Thus, there is growing evidence that the Z isomers are particularly prone to heterolysis when protonated at some sites, particularly $N_3$, and that equilibrium structures cannot be determined.

The effect of protonation at various sites on critical bond lengths is shown in Figures 4 and 5. Figure 4, a and b, display the optimized $N_1$–$N_2$ and $N_2$–$N_3$ bond lengths for all neutral and protonated conformations that produced stable protonated forms at the 3-21G level. Figure 4a shows that protonation on $N_3$ of the E isomers greatly increases the $N_2$–$N_3$ bond length (as it did in triazene and the methyltriazenes).[6] Though some of these are extremely long bonds, the positive frequencies indicate that they are still local energy minima and, therefore, intermediates rather than transition states. The effect of protonation of the oxygen in the E isomer also produced an increase in the $N_2$–$N_3$ bond length, but to a lesser extent than that caused by $N_3$ protonation. In the Z isomers protonation of the carbonyl oxygen produced a striking increase in the $N_2$–$N_3$ bond length. The most pronounced effect was seen in the (Z,syn,trans) isomer; the $N_1$–$N_2$ bond lengths became smaller than 1.2 Å as $N_2$–$N_3$ expanded to almost 1.7 Å. Such an extreme change in geometry suggests that the molecule could be on its way to the products of $N_2$–$N_3$ cleavage.

Table VI. Linear Fit Parameters[a] for Proton Affinities Scaling, Comparing AM1 Results with ab Initio Results

| triazene substituents compared | slope[a] (m) | *y*-intercept[a] (*b*) (kcal/mol) | std dev (kcal/mol) | correlation coefficient, *R* |
|---|---|---|---|---|
| *E*-acetyl | 1.577 | −103.4 | 6.2 | 0.979 |
| *Z*-acetyl | 1.603 | −98.4 | 30.6 | 0.773 |
| alkyl[b] | 1.044 | 25.2 | 23.6 | 0.953 |

[a] Fit to $y_{PA} = mx_{PA} + b$, for $x_{PA}$ = (AM1 proton affinity) and $y_{PA}$ = (3-21G proton affinity). [b] Data from ref 6 and 14.

Figure 5, a and b, compares the effect of protonation upon the $N_2$–$N_3$ and $N_3$–C bond lengths. These data provide information on the propensity of $N_2$–$N_3$ cleavage versus $N_3$–C cleavage. Figure 5a shows that protonations at $N_3$ of the E isomers produce an increase in the $N_2$–$N_3$ bond but also a comparable increase in the $N_3$–C bond length. Figure 5b shows that protonations on the carbonyl oxygen of the Z isomer produce a notable shortening of the $N_3$–C bond length, as the $N_2$–$N_3$ bond length increases to lengths larger than an average N–N single bond. Thus, although both the $N_3$–C and the $N_2$–$N_3$ bonds are lengthened significantly when protonation occurs at $N_3$, only the $N_2$–$N_3$ bond length is significantly longer when the protonation occurs on oxygen.

**3. Proton Affinities.** The numerical values for the ab initio proton affinities for each of the conformations of acetyltriazene at each protonation site are given in Table IV. Figure 6a graphically shows some important trends in the proton affinities of the E isomers. This figure also includes the proton affinities of unsubstituted triazene and some methyltriazenes.[6] In all but one case, proton affinities of 3-acetyltriazene are reduced from those of the other comparable triazenes. The one exception arises with the $N_1$-protonated (E,syn,cis) conformer, which was discussed above as being anomalously stable in the gas phase owing to intramolecular hydrogen bonding. This result is, therefore, consistent with the experimental findings that acylated triazenes are more stable in acid than their unacylated analogues.[12]

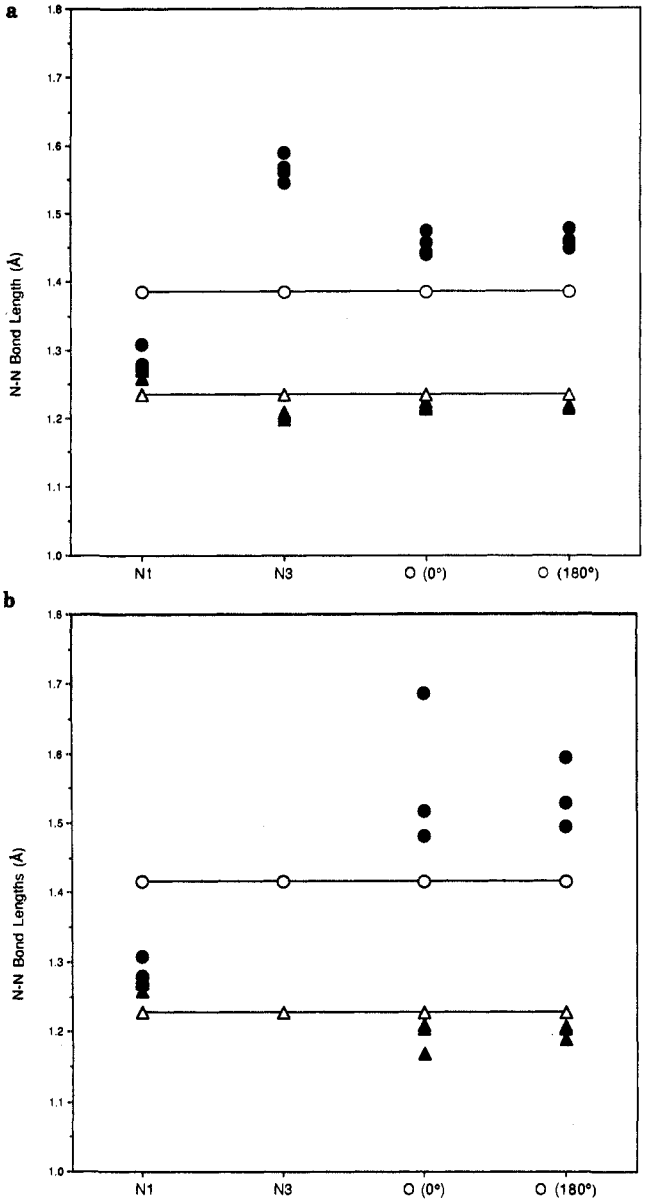


**Figure 4.** All optimized $N_1$–$N_2$ (▲) and the $N_2$–$N_3$ (●) bond lengths for each protonation site of (a) (*E*)-3-acetyltriazene and (b) (*Z*)-3-acetyltriazene. The lines with open symbols represent the respective average bond lengths for the neutral isomer.

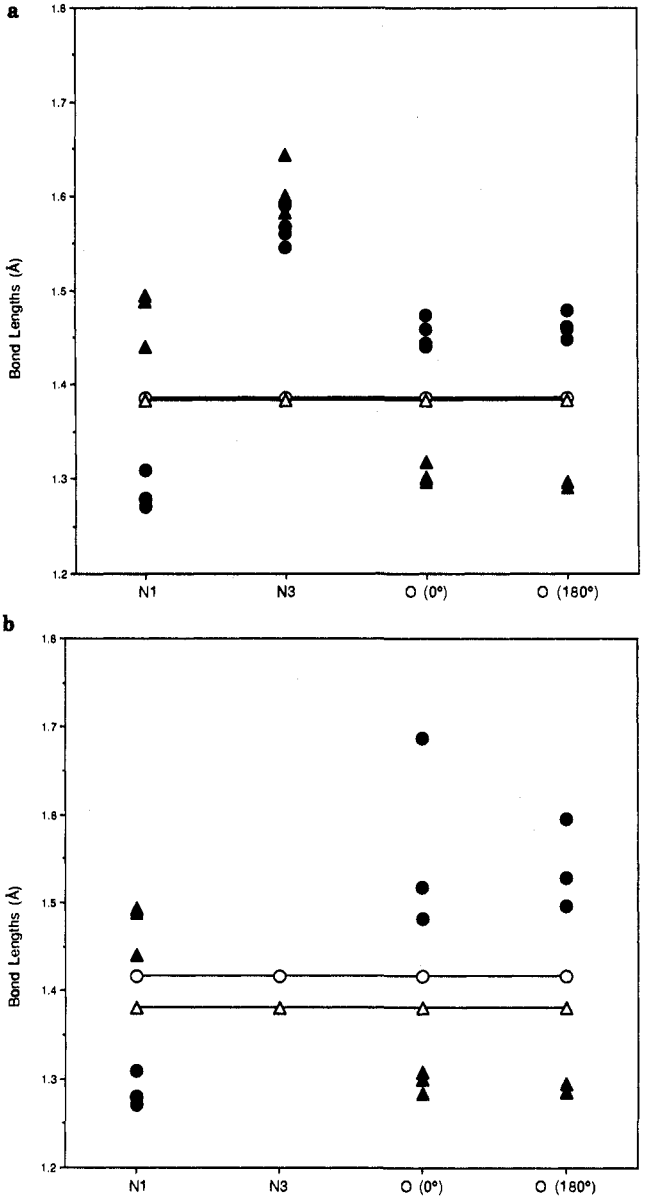


**Figure 5.** All optimized $N_2$–$N_3$ (●) and the $N_3$–C (▲) bond lengths for each protonation site of (a) (*E*)-3-acetyltriazene and (b) (*Z*)-3-acetyltriazene. The lines with open symbols represent the respective average neutral bond lengths.

Throughout the triazene analysis we see that the $N_3$ proton affinity is significantly smaller than that of the other three protonation sites studied in 3-acetyltriazene here, making it less competitive as the site of initial protonation.

Interestingly, Figure 6a shows that oxygen protonations are competitive with protonation on $N_1$. In fact, except for the (E,syn,cis) conformer, oxygen protonation is slightly more energetically favorable. In view of the finding that O-protonation increases the $N_2$–$N_3$ bond length, this result suggests that O-protonation leads to dissociation. $N_1$ of the (E,syn,cis) conformer is an exceptionally good protonation site (see Figure 2c). One can see that protonation at both $N_1$ and $O_{(0°)}$ for this conformer can take advantage of a six-membered ring intramolecular hydrogen bond. But since protonation at each site provides different optimized structures, the intramolecular hydrogen bonding appears to be asymmetric. The $N_1$ proton affinity is slightly larger than $O_{(0°)}$ proton affinity for this conformation. In the $N_1$ protonated structure, the nonbonding distance between the new proton and oxygen is 1.84 Å, and in $O_{(0°)}$ protonation, the nonbonded distance between the new proton and the $N_1$ is 1.80 Å. Since oxygen is a larger atom than nitrogen by approximately 0.04 Å, the two nonbonding distances should be considered of comparable length.

Figure 6b shows the Z-isomer's proton affinity trends for those conformations that produced stable protonated products. The proton affinities for the $N_1$ site are higher than those at the oxygen sites; similarly, ab initio results predict $N_1$ protonation to be preferred over oxygen protonation, by 7 to 16 kcal/mol.

**B. Relating the ab Initio RHF Results to the Results of AM1.** An in-depth comparison of the semiempirical AM1 to the ab initio 3-21G results has been made to assess the reliability of predicting 3-21G results from AM1 calculations. Our interest in this comparison stems from our intention to study larger triazenes at the lowest possible calculational level that will give reliable trends. Prior work has shown that the 3-21G basis results will be large compared to the actual experimental values for proton affinity, but that the trends in proton affinities are accurately reproduced.[6,19] In unsubstituted triazene and methyltriazene, 3-21G proton affinities are parallel in trend compared to those calculated with the 3-21G$^+$ basis set which includes some extra polarization functions. Calculations show that proton affinities obtained with 3-21G$^+$ basis compare favorably with experiment.[19] It has been argued that the extra polarization functions in the "plus" basis set have the extra flexibility necessary to correctly describe protonation. In unsubstituted triazene and methyltriazenes, 3-21G

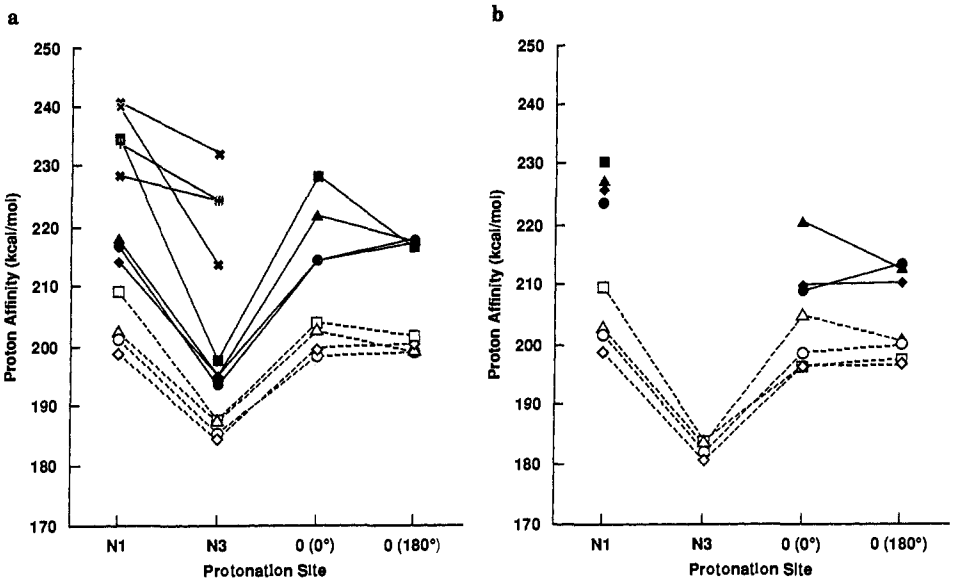


**Figure 6.** The optimized RHF 3-21G (—) and AM1 (---) proton affinities for each protonation site of (A) the E isomers of unsubstituted triazene (+), methyl- and dimethyltriazenes[6] (×), and the four conformers of 3-acetyltriazene and (b) the Z isomers of the four conformers of 3-acetyltriazene [(▲), (●), (■), and (♦) for (anti,cis), (anti,trans), (syn,cis), and (syn,trans), respectively].

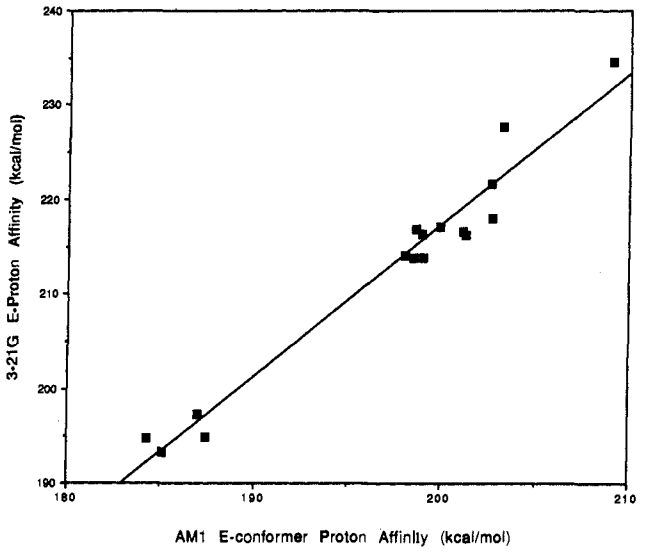


**Figure 7.** A comparison of the optimized proton affinities calculated using AM1 energies with those calculated by using ab initio energies (RHF at the 3-21G level) for (*E*)-3-acetyltriazene. The line represents the least-squares fits of the data (see Table V1).

results are parallel in trend to 3-21G$^+$.[19] Therefore, we have confidence that our 3-21G results yield correct conclusions on the relative proton affinities reported here.

Figure 7 shows that good agreement exists between AM1 and 3-21G proton affinities for all four protonation sites of the four E isomers of acyltriazene with two exceptions. The two points which noticeably diverge from the line both involve the (E,syn,cis) conformer. This one anomalous conformer was identified earlier as a special case due to the involvement of intramolecular hydrogen bonding, widely known to be poorly treated by AM1. So, except for this case, the AM1 proton affinities for the E isomers are in good agreement with the 3-21G results. The 10 optimized Z isomers of acetyltriazene, however, show a much poorer correlation between the two methods. Furthermore, AM1 has always predicted stable protonations on $N_3$ when ab initio results are unable to locate a stationary state. The Z isomers, especially those that did not optimize, have a characteristically longer $N_2$–$N_3$ bond. We conclude that there is agreement in proton affinity among the two calculations when the molecule has a typical $N_2$–$N_3$ bond length, hence when it is not showing signs of instability at that bond. However, AM1 appears to overestimate the stability of conformations, giving artificially short $N_2$–$N_3$ bonds and stable optimized structures for conformers that the 3-21G calculations suggest are headed toward heterolysis.

In this analysis, we show that the correlation between bond lengths in AM1 and 3-21G involves a linear scaling. We use the results of this analysis to provide empirical predictions for estimating N–N and N–C bonds. Linear functions applied to the AM1 optimized triazene N–N and N–C bonds can predict bond lengths produced by the 3-21G calculation, with fair accuracy (see Figure 8):

$$Y_{\text{NN bond}} = 1.467X_{\text{NN bond}} - 0.567 \text{ Å} \quad (4a)$$

$$Y_{\text{NC bond}} = 1.418X_{\text{NC bond}} - 0.616 \text{ Å} \quad (4b)$$

where $X_{\text{bond}}$ is the AM1 bond length and $Y_{\text{bond}}$ is the 3-21G length prediction. The slope and intercept parameters for N–C are fairly close to those determined for N–N. In all cases it is evident that the parametric fit starts to break down most noticeably at the largest bond lengths, where AM1 geometries cease to lengthen as their ab initio counterparts continue to grow.

Though the AM1 ab initio correlation between N–N and N–C bond lengths was quite promising, an identical approach to predict 3-21G values of bond angles was unsuccessful. There was no significant correlation between the two calculational methods for values of bond angles. Thus, it appears that nitrogen bond lengths are the only safe parameter to which we may apply a scaling formula on the AM1 results to predict 3-21G optimized geometries. But, since the $N_2$–$N_3$ and the $N_3$–C bonds are of greatest interest in our current study of heterolysis, the reduced ability of AM1 scaling to reproduce bond angles is not detrimental to our objective. Currently we are using the bond-length scaling to predict 3-21G input values, providing us accelerated convergence of the 3-21G calculations.

## IV. Conclusions

Acetyltriazene was chosen as the prototype acyltriazene, several of which are under active study as possible antitumor agents.[4] It has been shown experimentally that acyltriazenes decompose in aqueous solutions by three different mechanisms, depending on the pH of the medium. The acid-catalyzed reaction occurs over the pH range of 0–5. Between pH 5 and 9.5 there is an uncatalyzed domain, and at pH >9.5 base catalysis is observed. The present quantum mechanical study was designed to provide a theoretical framework for the experimental kinetic data and product studies of the acid-catalyzed reaction. We also hoped to provide a basis for structure–activity properties of unknown compounds.

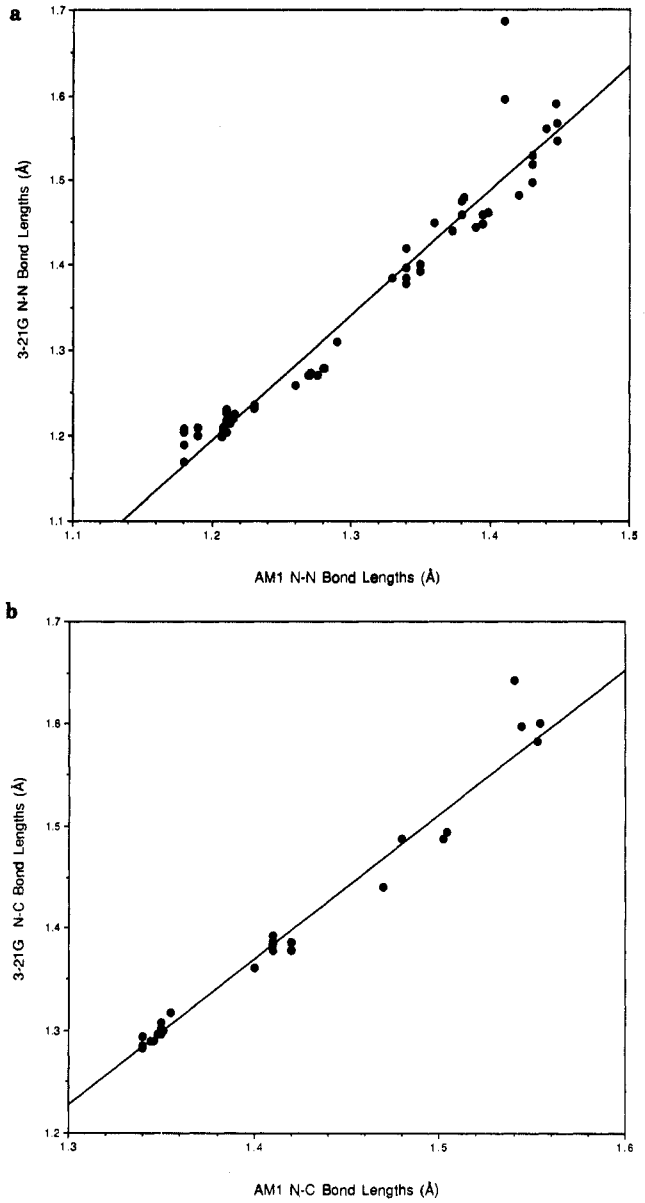


**Figure 8.** (a) A comparison of the N–N bond lengths calculated by AM1 with those calculated by ab initio (RHF at the 3-21G level). (b) A comparison of the N–C bond lengths calculated by AM1 with those calculated by ab initio (RHF at the 3-21G level). The lines represent the least-squares fits of the data (see eq 4a and 4b.)

Previous quantum mechanical studies on triazene and various methyl triazenes demonstrated that protonation of the saturated nitrogen, $N_3$, in $RN_1{=}N_2{-}N_3R'R''$ predisposes the molecule to heterolysis by lengthening the $N_2$–$N_3$ bond. These earlier studies also show that the protonation of the Z isomer of triazene led to synchronous scission of the $N_2$–$N_3$ bond; i.e., no stable $N_3$-protonated structure could be detected. The present study shows that acyltriazenes, as exemplified by acetyltriazene, share some characteristics in common with alkyltriazenes but also exhibit significant differences in properties. Calculations at the 3-21G level show that protonation of the Z isomer of acetyltriazene on $N_3$ failed to converge to a stable structure. This, of course, does not preclude the possibility that convergence could be achieved by using a larger basis set, particularly if configuration interaction was included. Nevertheless, the lack of convergence at the 3-21G level suggests that $N_3$ protonation (*Z*)-acyltriazene would lead to heterolysis of the $N_2$–$N_3$ bond. We found here, however, that the $N_3$-protonation in general is a high-energy process. Instead, O-protonation along with $N_1$-protonations are the most likely reactions. For reasons discussed earlier,[6] $N_1$ protonation is not likely to be important as a productive pathway of hydrolysis. Thus, the acid-catalyzed hydrolytic decomposition of acetyltriazene, and by extension the acid-catalyzed hydrolytic decomposition of other acyltriazenes, involves O-protonation as the first step in the hydrolytic reaction. O-protonation also results in the lengthening of the $N_2$–$N_3$ bond (Table III), although this effect is not quite as pronounced as in the $N_3$ protonations. The O-protonation does not involve an increase in the $N_3$–C bond length. Thus, a prediction could be made that the acid-catalyzed hydrolysis of acetyltriazene would involve $N_2$–$N_3$ bond cleavage and no $N_3$–C bond cleavage. This is exactly what is observed experimentally.

The ab initio RHF calculations in this paper were restricted to the 3-21G level. While this basis set produces reliable geometric information, the energy parameters are frequently too high. We had previously determined, however, that the energy trends were reasonably well correlated between 3-21G and the more accurate basis sets such as 3-21G$^+$, 6-31G* and MP3/6-31G*.[6,19] So while we have little confidence in the absolute value of the proton affinities reported in Table IV, we feel that the trends between the various values are realistic.

It was gratifying to find a surprisingly good correlation between bond lengths calculated by ab initio RHF methods and those obtained by scaling the results of a semiempirical AM1 calculation. A linear scaling procedure was applied successfully to the AM1 optimized N–N and N–C bonds in the triazenes, which shows promise as a predictor for ab initio bond lengths. This scaling, however, does not hold well for bond angles and therefore must be used with some caution. A good linear scaling was found for relating the AM1 and ab initio proton affinities for relatively stable conformers of acetyltriazene. However, this scaling was relatively inaccurate for the more reactive (*Z*)-triazenes and, of course, failed completely for those cases where no stable cationic intermediate was optimized at the 3-21G level. The AM1 calculations converged on a stable intermediate in all cases. We are currently using the bond-length scaling to predict ab initio input values, which provides an accelerated convergence of the ab initio RHF calculations.

**Acknowledgment.** We are grateful to the National Cancer Institute's Advanced Scientific Computing Laboratory for generous amounts of CPU time on the Cray XMP-2 supercomputer. J.L.O. and A.M.S. wish to acknowledge the assistance of Kristian Witt. This research is sponsored in part by the National Cancer Institute, DHHS, under Contract No. NO1-CO-74101 with BRI. Partial support for R.H.S. was derived from N.S.F. Grant CHE-8521385.